



## EUROGAM - A High Efficiency Escape Suppressed Spectrometer Array

P. J. NOLAN  
Oliver Lodge Laboratory  
University of Liverpool  
Liverpool  
L69 3BX

### 1. Introduction

EUROGAM is a UK-France collaboration to develop and build a high efficiency escape suppressed spectrometer array. The project has involved the development of both germanium (Ge) and bismuth germanate (BGO) detectors to produce crystals which are both bigger and have a more complex geometry. As a major investment for the future the collaboration has developed a new electronics and data acquisition system based on the VXI and VME standards. The array will start its experimental programme in mid 1992 at the Nuclear Structure Facility at Daresbury, U.K. At this stage it will have a total photopeak efficiency (for 1.33 MeV gamma-rays) of ~4.5%. This will give an improvement in sensitivity (relative to presently operating arrays) of a factor of about 10. When EUROGAM moves to France in mid 1993 its photopeak efficiency will have increased to about 8.5% which will result in an increase in sensitivity of a further factor of about 10. In this article I will concentrate on the array which will operate at Daresbury in 1992 and only briefly cover the developments which will take place for the full array before it is used in France in 1993.

### 2. Detector Developments

The detector module to be used in the first phase of EUROGAM is shown in Figure 1. It consists of a large n-type hyperpure Ge detector surrounded by a BGO escape suppression shield. The high resolution Ge detector is tapered over the front 30 mm of its length to allow for closer packing when in the array. The detectors to be used in EUROGAM typically have (for 1.33 MeV gamma-rays) a resolution of 2.1 keV and a relative efficiency of 75%. The BGO detectors are divided into 10 optically isolated elements, each with a photomultiplier readout. The complex shape of the detectors can be seen in the diagram shown in Figure 2. The individual BGO elements have resolutions (for 662 keV gamma-rays) of 18 - 22% when the source is placed in the germanium detector position. For its initial operation EUROGAM will consist of 45 of the detector modules shown in Figure 1.

A new four element detector is being developed for the second phase of EUROGAM. The detector shape is shown schematically in Figure 3. The improved granularity of this detector will help reduce Doppler broadening, especially when it is positioned at 90° to the beam direction. The properties and status of this detector are discussed in more detail in the contribution of Duchêne<sup>1)</sup> (also in this proceedings).

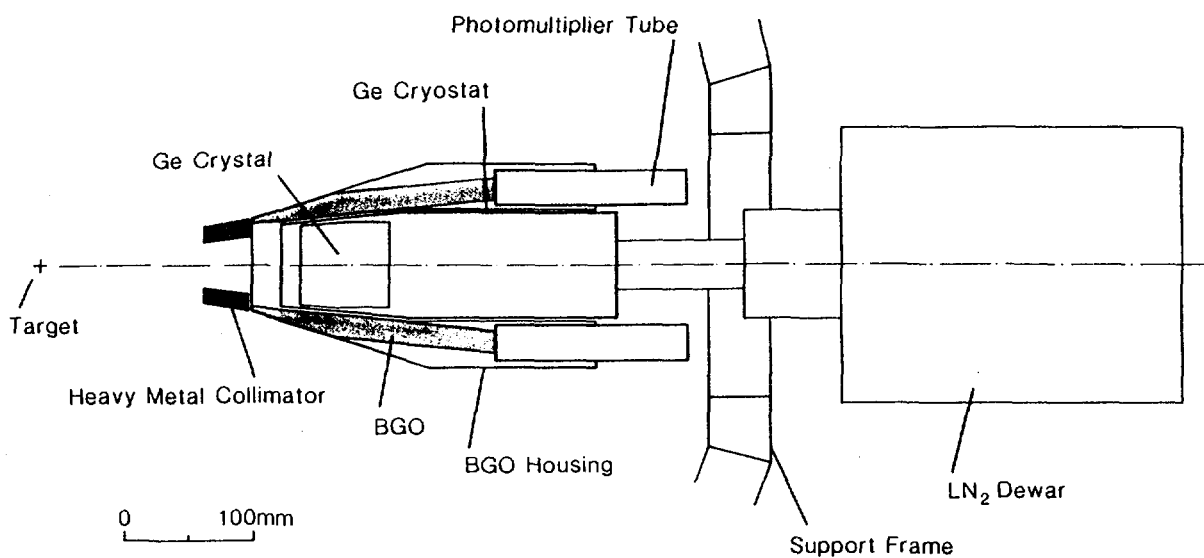


Figure 1 The escape suppressed spectrometer to be use in the first phase of EUROGAM.

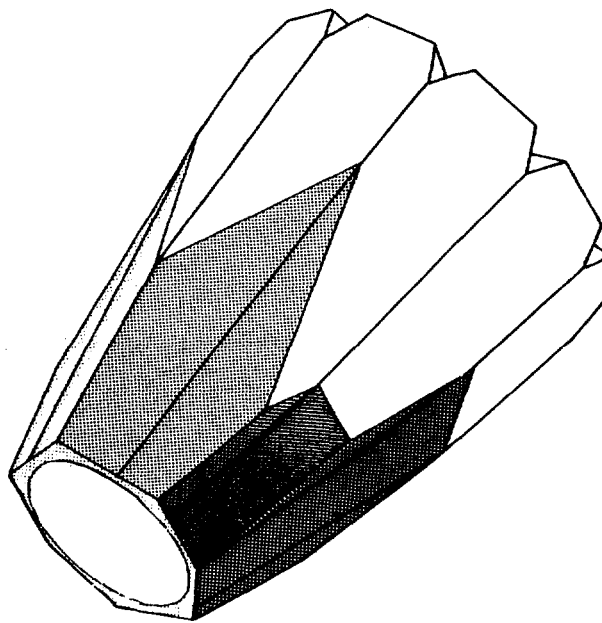


Figure 2 Schematic drawing of the BGO shield to be used in EUGOGAM. It consists of 10 optically isolated elements.

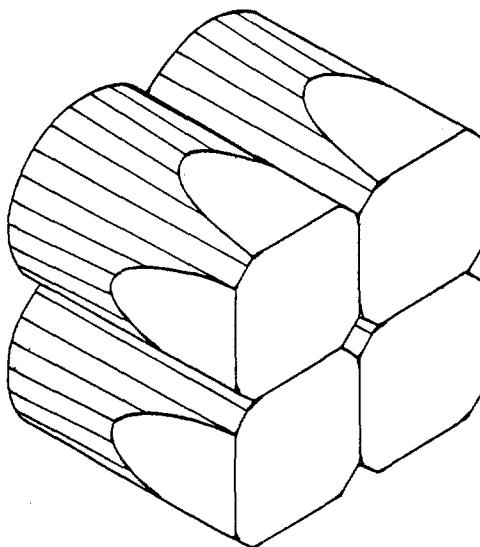


Figure 3 The four element clover detector being developed for EUROGAM phase 2.

### 3. Measurements on the Prototype Detectors

An extensive set of measurements has been carried out both with sources and in-beam for a 'mini' array of five escape suppressed spectrometers. These were all of the type shown in Figure 1. The results of these tests have been published<sup>2)</sup> and will be discussed briefly here.

The design of an escape suppressed array has to incorporate many features. These include a high photo-peak detection efficiency, a good response function and a low cost. Achieving these aims means that many items need to be considered. It is the optimisation of all of these that leads to a successful design. In the test measurements a number of these items have been measured. These include the effects of isolated hit probability, reduced efficiency due to neutrons and random vetoes from the suppressors, peak to total and Doppler broadening. All except the latter will be discussed in the next paragraphs. The Doppler broadening measurements are discussed by Duchêne<sup>1)</sup>.

A schematic diagram showing the arrangement of the detectors for the tests is shown in Figure 4. The peak to total for  $^{60}\text{Co}$  measured for shield A is 55 - 59% (depending on the Ge detector used) when only its surrounding shield is used as a suppressor (individual suppression). In shared suppression mode (using also the surrounding shields as indicated) this value increased to 63 - 65%. Two shared suppression modes were tried. In the first (mode 1) no account was taken of whether germanium detectors B - G also fired. In the second (mode 2) the event was not rejected if a second germanium fired. No major difference was found in the peak to total for the two modes. For  $^{137}\text{Cs}$  typical peak to total values are 70% (individual suppression) and 73% (shared suppression).

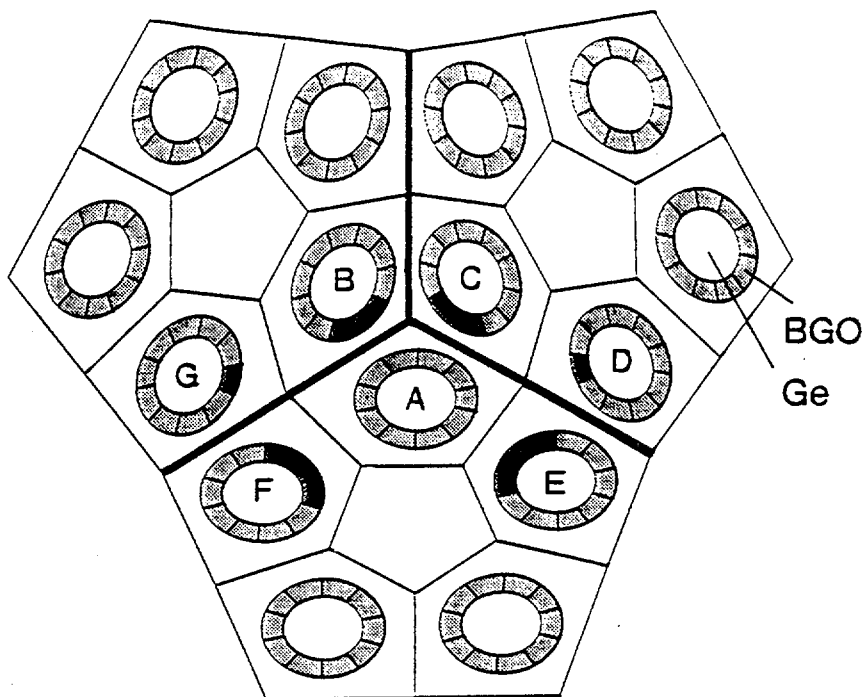


Figure 4 Schematic diagram of the detector arrangement for the test experiments

The amount of data lost was also measured. This is the intensity of a photopeak when a suppressed spectrum was compared to an unsuppressed spectrum. The data were taken following the  $^{100}\text{Mo} + ^{32}\text{S}$  reaction at a beam energy of 132 MeV where the gamma-ray multiplicity is expected to be  $\sim 15$ . The data are shown in Figure 5. There are two causes of losses in this case. The first is due to bad vetoes from the suppressors due to scattered gamma-rays. This should depend on gamma-ray multiplicity. The second is bad vetoes due to neutrons hitting the suppressors. This will depend on the neutron multiplicity. The data confirm that at forward angles the loss rate is higher due to the forward peaking of neutrons in this reaction.

The effect of gamma-ray multiplicity can be measured with sources. Full details of the method are given by Beausang et al<sup>2)</sup>. The results are shown in Figure 6. These data show that for multiplicity 30 (1.33 MeV gamma-rays) the loss rate is between 10% and 23% depending on the suppression mode used. The expected losses for multiplicity 15 are 5%, 8% and 12% for individual, shared suppression 2 and shared suppression 1 respectively. These are in good agreement with the measured in beam loss rates (at background angles) of 5%, 8% and 10% respectively for the three modes. The additional loss rates at forward angles are due to the effect of neutrons.

An additional loss of photopeak events arises from the isolated hit probability. That is the effects of more than one gamma-ray hitting a particular detector. This effect was again measured by sources<sup>2)</sup>, the results being shown in Figure 7. There is an additional 12% loss in the photopeak intensity for multiplicity 30.

The combination of peak to total and loss rates needs to be considered for individual experiments before deciding on the best mode of operation.

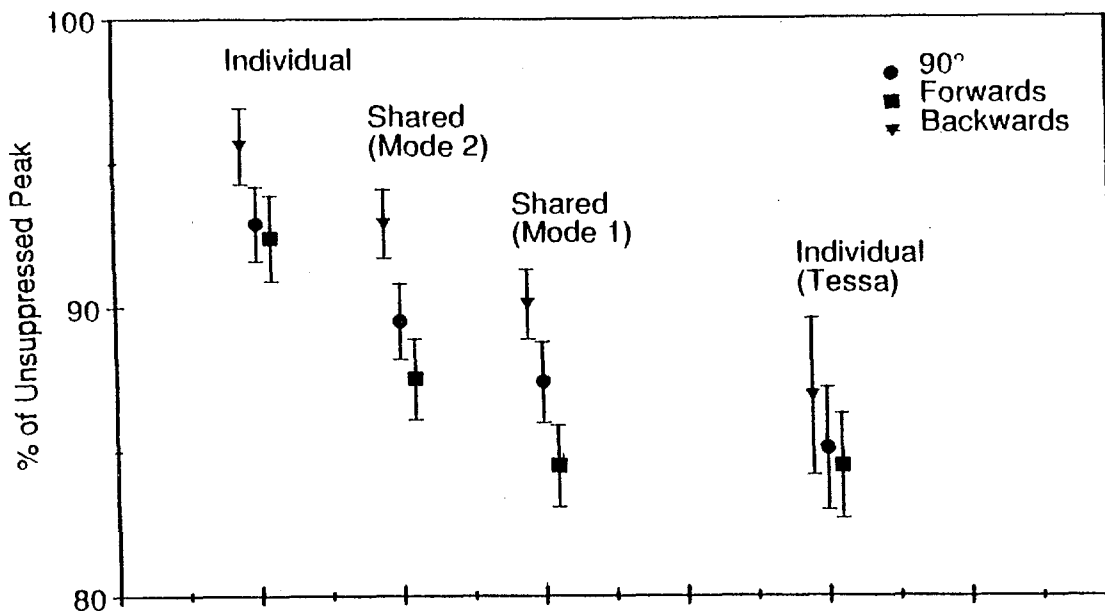


Figure 5 Comparison between suppressed and unsuppressed spectra to determine loss rates due to suppression. The terms are defined in the text. The forward angle used was 72°, the backward angle used was 158°.

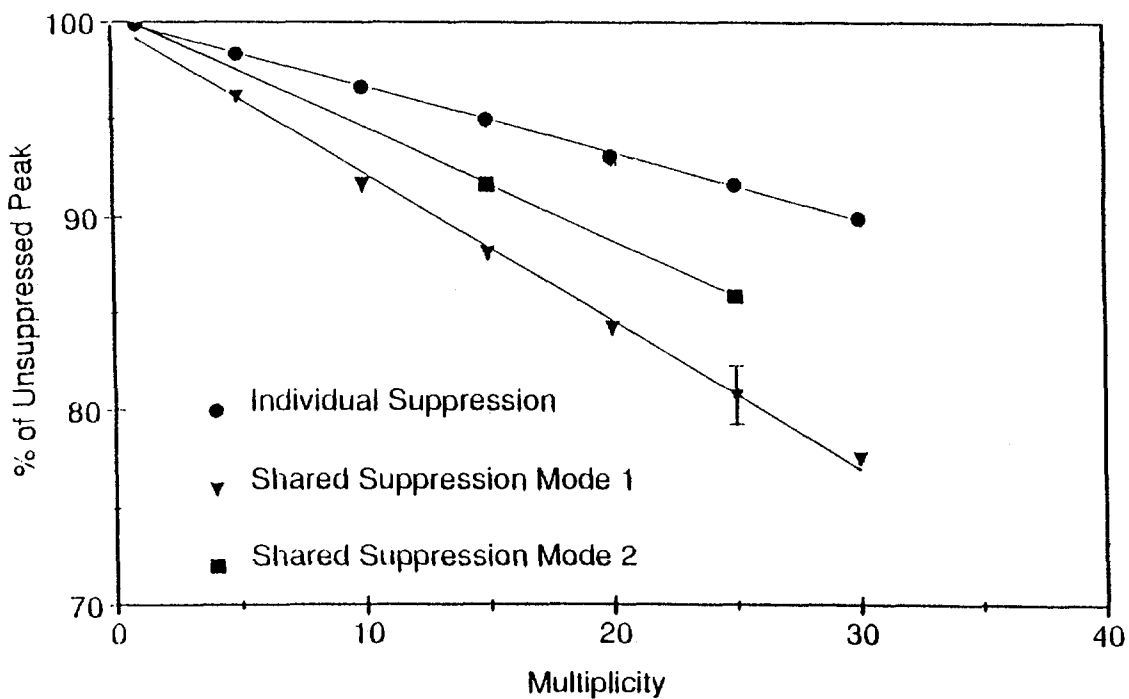


Figure 6 Percentage of unsuppressed peak area remaining in various suppressed spectra as a function of gamma ray multiplicity. A  $^{60}\text{Co}$  source was used.

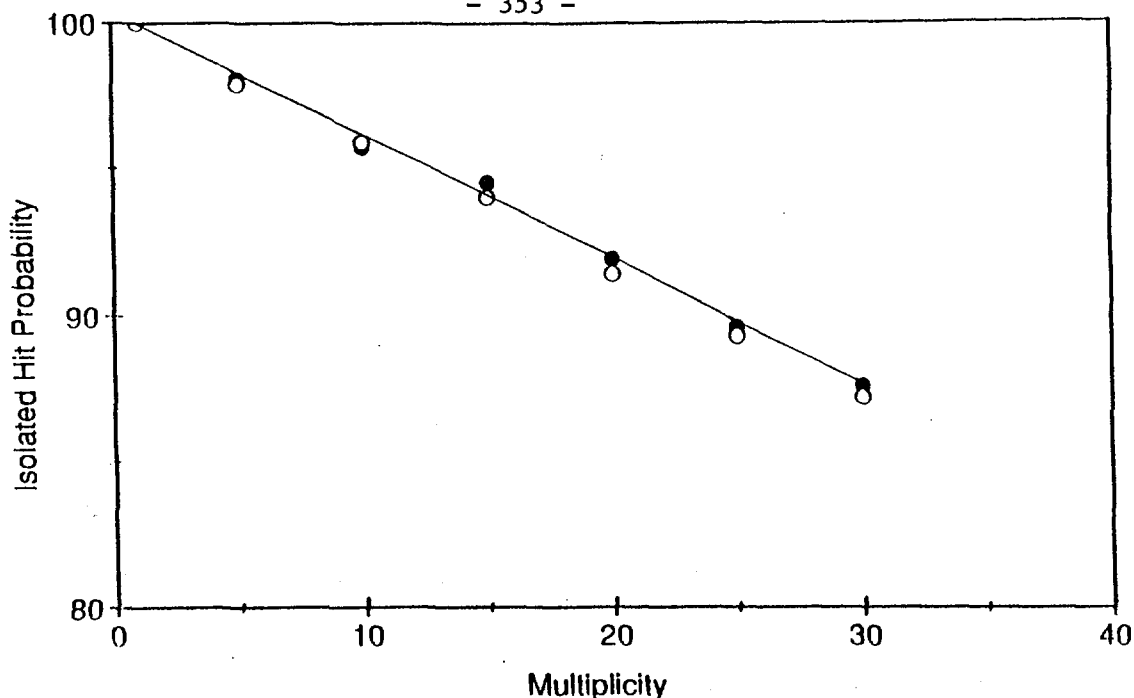


Figure 7 Isolated hit probability measured (see text) as a function of gamma ray multiplicity for  $^{60}\text{Co}$  (1.33MeV) and  $^{207}\text{Bi}$  (0.57MeV).

#### 4. System Commissioning Tests

A series of in-beam commissioning tests were carried out using 25 - 30 escape suppressed detectors with conventional NIM electronics. One of these will be reported briefly here, others are discussed by Duchêne<sup>1)</sup> and Hannachi<sup>3)</sup>.

The superdeformed band<sup>4)</sup> in  $^{132}\text{Ce}$  was populated using the  $^{100}\text{Mo} (^{36}\text{S},4n) ^{132}\text{Ce}$  reaction at a beam energy of 150 MeV. For this experiment 27 EUROGAM detectors were used at the following angles: 7 @ 134°, 12 @ 108°/72°, 8 @ 94°/86° (note the other angles available in EUROGAM are 158°/22° and 46°).

The measured experimental rates are given in Tables 1 and 2 for a target thickness of  $0.5 \text{ mg cm}^{-2}$  and a beam current of 2 pA.

**Table 1** Measured Detector Rates

| <u>Angle</u><br>(Deg) | <u>Unsuppressed</u><br>(kHz) | <u>Ge</u><br><u>Suppressed</u><br>(kHz) | <u>BGO</u><br>(kHz) |
|-----------------------|------------------------------|---|---------------------|
| 134                   | 2.7                          | 1.4                                     | 0.28                |
| 108                   | 2.8                          | 1.5                                     | 0.34                |
| 94                    | 2.7                          | 1.3                                     | 0.33                |
| 86                    | 2.5                          | 1.2                                     | 0.39                |
| 72                    | 2.5                          | 1.2                                     | 0.44                |

**Table 2** Measured and Predicted Coincidence Rates

| <u>Fold</u> | <u>Measured*</u><br>(27 Ge)<br>(kHz) | <u>Predicted**</u><br>(45 Ge)<br>(kHz) |
|-------------|--------------------------------------|--|
| ≥2          | 7.2                                  | 59                                     |
| ≥3          | 2.3                                  | 29                                     |
| ≥4          | 0.55                                 | 11                                     |
| ≥5          | 0.10                                 | 3                                      |
| ≥6          |                                      | 0.7                                    |

\* beam 2pnA

\*\* beam 8pnA giving a singles unsuppressed Ge rate of ~10 kHz

Sum of 2-d gates: Background subtracted

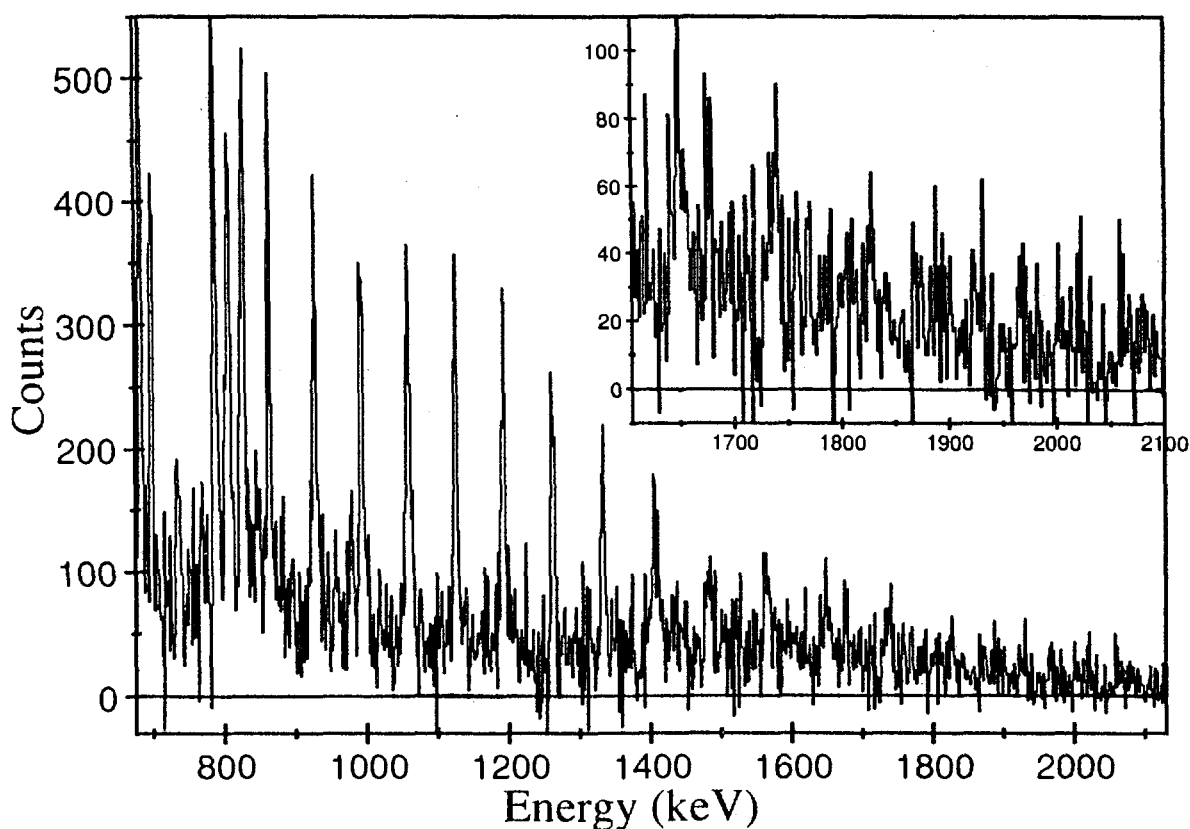


Figure 8 Spectrum (derived from triples data) of the superdeformed band in  $^{132}\text{Ce}$  in coincidence with 13 pairs of gates on transitions in the superdeformed band.

The higher fold coincidence events can be unfolded to give many doubles, triples etc. The predicted figures given on Table 2 result in the following unfolded rates: triples 86 kHz, Quadruples 32 kHz, quintuples 9 kHz etc. In about 100 hours of beam time the data set available will be  $\sim 3 \times 10^{10}$  triples and  $\sim 1.1 \times 10^{10}$  quadruples.

The  $^{132}\text{Ce}$  superdeformed band spectrum obtained in this experiment is shown in Figure 8. All the previously seen transitions are in the spectrum with approximately

the same peak to background. EUROGAM data was taken in about 4 hours of beam time (assuming 8 pA) while the original TESSA3 data were collected in about 100 hours of beam time.

5. Electronics and Data Acquisition

The layout of the system is shown in the schematic diagram in Figure 9. The signals from the detectors are processed in VXI based electronics. The Germanium VXI based card takes signals from 6 detectors and outputs two energies (0 - 4 MeV and 0 - 20 MeV), a time based on a constant fraction discriminator and a time based on a cross over circuit. The latter is used for pile up rejection and pulse shape analysis. The BGO VXI card takes signals from 60 BGO crystals and is designed to correspond to the channels in an adjacent Ge card. The BGO card outputs energy, time and the pattern of BGO crystals in an event. Also in VXI electronics are the Master Trigger (which controls the logic for the event), the Readout Controller and a Resource Manager. Components of the system are described in more detail in references 5 - 11.

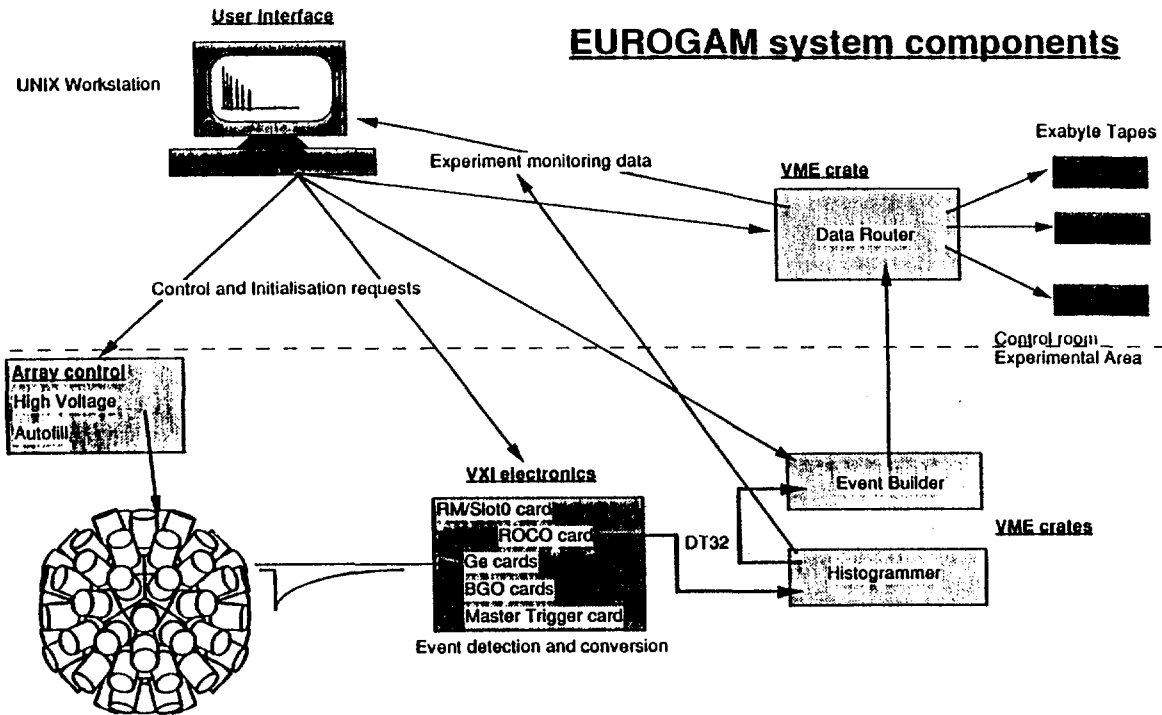


Figure 9 The EUROGAM electronics and data acquisition system

The data are read out from the VXI crate along a 32 bit bus into the data acquisition system which is VME based<sup>12)</sup>. A histogrammer module can produce spectra for all parameters flowing along this bus. The data are built into events using commercially available VME modules and then passed to the data sorter and data router. The latter allows different sub sections of the data (e.g. triples, quadruples etc) to be directed to different storage devices. The system is designed to handle a rate of ~ 2 Mbytes/sec, but can be upgraded to 5 - 6 Mbytes/sec.

All the above components have been tested (including the software) and work to specification. Currently (May 1992) the final system tests are underway.

In addition to the above a VME based control and monitoring system has been developed for the liquid nitrogen autofill system, the detector HV modules and the environmental monitoring.

## 6. Auxiliary Detectors

The power of a device like EUROGAM is enhanced when it is operated in conjunction with additional detectors. During the EUROGAM commissioning tests a downstream isomer detector and the Daresbury recoil mass separator<sup>13)</sup> have been used in coincidence with EUROGAM. In addition several other devices are being designed. These include gas detectors, an inner ball for some energy/multiplicity determination apparatus for recoil distance and g-factor measurements, neutron detectors etc.

As an illustration of the power of such devices some of the data taken using the recoil mass separator in coincidence with EUROGAM will be discussed. The  $^{104}\text{Ru} + ^{34}\text{S}$  reaction was used at a beam energy of 160MeV. The data recorded were multifold suppressed  $\gamma$ -coincidences (fold  $\geq 3$ ) and recoil -  $\gamma$  (fold  $\geq 2$ ) coincidences.

Figure 10 shows spectra corresponding to the known highly deformed band in  $^{133}\text{Nd}$ . The band can clearly be seen in both spectra, the mass gating reducing the contamination.

## 7. Current Status (May 1992)

The experimental programme on EUROGAM will start in summer 1992 using a system consisting of 45 detectors. This will have a photopeak efficiency (for 1.33 MeV gamma-rays) of ~ 4.5%. EUROGAM will move to France in summer 1993 and be upgraded to include some new 4 element clover detectors. The EUROGAM arrangement, shown in Figure 11, will then comprise 30 detectors from phase 1 (placed around  $0^\circ$  and  $180^\circ$ ) and 24 clover detectors (placed near  $90^\circ$ ). This array should have a total photopeak efficiency of ~8.5%.

## Acknowledgements

The EUROGAM collaboration is jointly funded in France by IN2P3 and in the UK by SERC. I would like to thank all those who have contributed to the EUROGAM project.

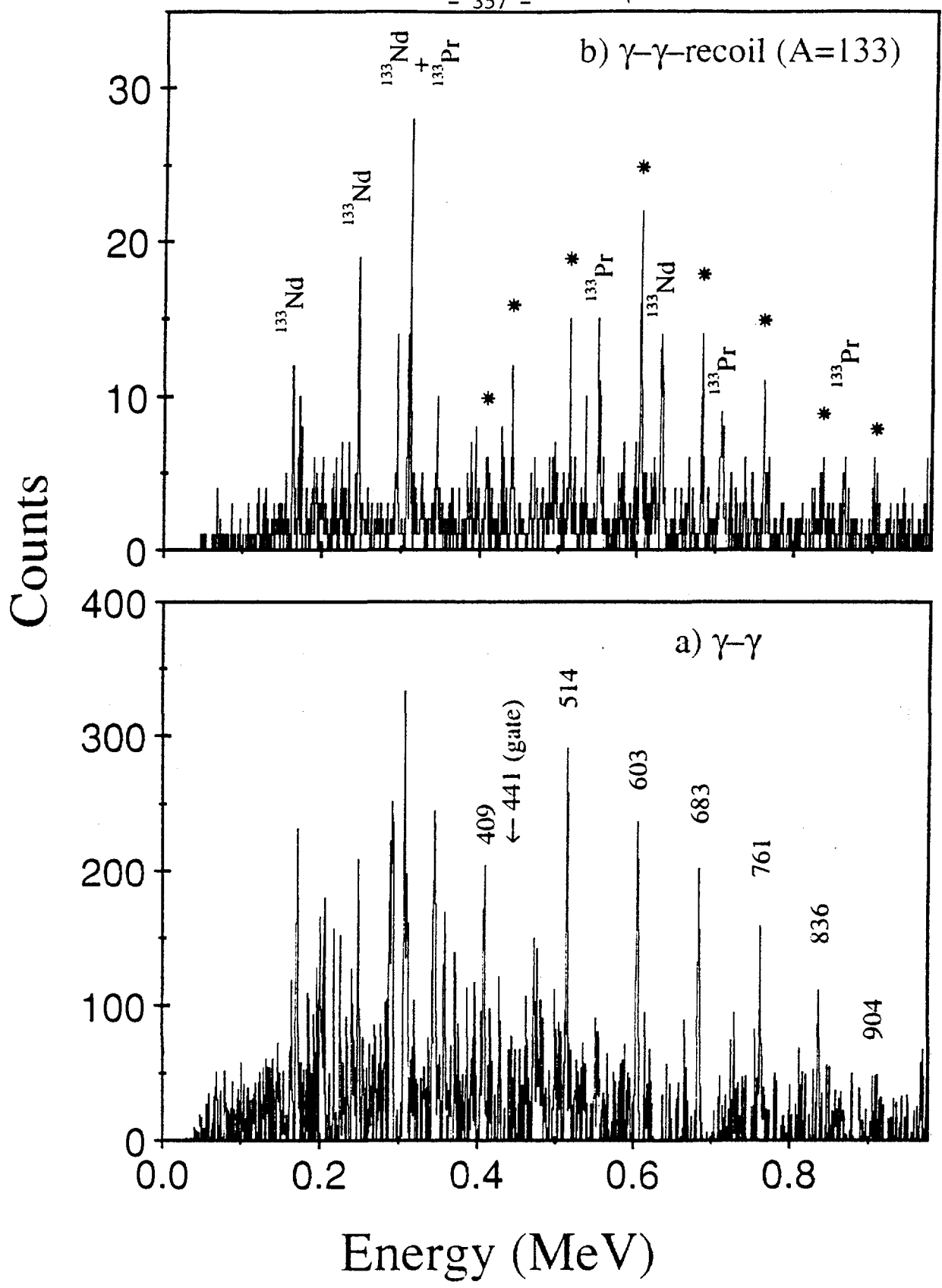


Figure 10 Spectra from  $\gamma\text{-}\gamma$  and mass (A=133) gated  $\gamma\text{-}\gamma$  data for the highly deformed band in  $^{133}\text{Nd}$ . (a) a single gate on the 441 keV transition, (b) a sum of gates on 6 transitions in the band. Members of the band are marked \*.

**References**

- 1) Duchêne G., Proceedings of the Workshop on Large Gamma-ray detector arrays, Canada May 1992 AECL 10613 (1992)
- 2) Beausang C. W. et al, Nucl. Instrum. Meth. A313 37 (1992)
- 3) Hannachi F., Proceedings of the Workshop on Large Gamma-ray detector arrays, Canada May 1992 AECL 10613 (1992)
- 4) Kirwan A. et al, Phys. Rev. Lett. 58 467 (1987)
- 5) Richard A. et al, IEEE Nuclear Science Symposium, New Mexico, USA, 1991
- 6) Bosson G. et al, IEEE Nuclear Science Symposium, New Mexico, USA, 1991
- 7) Poux J., IEEE Nuclear Science Symposium, New Mexico, USA, 1991
- 8) Berst J. et al, IEEE Nuclear Science Symposium, New Mexico, USA, 1991
- 9) Lazarus I. et al, IEEE Nuclear Science Symposium, New Mexico, USA, 1991
- 10) McPherson G. M. et al, IEEE Nuclear Science Symposium, New Mexico, USA, 1991
- 11) Alexander J. et al, IEEE Nuclear Science Symposium, New Mexico, USA, 1991
- 12) Pucknell V. and Aleonard M. M., Proceeding of the Real Time 91 Conference, Julich, Germany 1991
- 13) James A. N. et al, Nucl. Instrum. Meth. A267 144 (1988)